

Self-optimization, community stability, and fluctuations in a class of individual-based models of biological coevolution

Per Arne Rikvold

*School of Computational Science, Center for Materials Research and Technology,
National High Magnetic Field Laboratory, and Department of Physics,
Florida State University, Tallahassee, Florida 32306-4120, USA
and Department of Fundamental Sciences, Faculty of Integrated Human Studies,
Kyoto University, Kyoto 606, Japan*

Abstract

We study a class of individual-based models of biological coevolution. These are multispecies, stochastic population-dynamics models in which the reproduction probability for individuals of a particular species depends nonlinearly on the population sizes of all the species present in the community. New species are introduced through a small probability of mutation during reproduction. For a subclass of simplified models we are able to perform linear stability analysis, and we compare the analytic results with large-scale kinetic Monte Carlo simulations. Based on this analysis, we present a phase diagram for the total population size. Over time, the models are found to *self-optimize* through mutation and selection to maximize a community fitness function, subject only to constraints internal to the model. If the off-diagonal elements of the matrix that defines the interspecies interactions are distributed independently on an interval that includes positive values, the model evolves toward *mutualistic* communities, in which the population is self-sustaining. In contrast, for predator/prey models the interaction matrix is antisymmetric, and the community is constrained to a region of the phase diagram where a nonzero population size can only be sustained by an external resource. Time series of the diversity and total population size for the different models show $1/f$ noise and power-law distributions for the lifetimes of communities and species. For the mutualistic model, these two lifetime distributions have the same exponent, while their exponents are different for the predator/prey model. The difference is probably due to a greater resilience of the predator/prey model toward mass extinctions.

Key words: Evolution, Self-optimization, Community stability, Mutualistic interactions, Predator-prey interactions, Power laws

1 Introduction

Traditionally, problems in ecology and evolution have been addressed at very different levels of resolution. Typically, ecological problems are addressed on a timescale of generations and often at the level of individual organisms, while issues in evolution are considered on much longer, often geological, timescales and usually at the level of species or even higher-level taxa. However, in recent years it has been recognized that processes at the ecological and evolutionary scales can be strongly linked (Thompson, 1998, 1999; Drossel et al., 2001; Yoshida et al., 2003). Several models have therefore been proposed, which aim to model the resulting complex problem of coevolution in a fitness landscape that changes with the composition of the community, while spanning the disparate scales of both temporal and taxonomic resolution. Among these models are the Webworld model (Caldarelli et al., 1998; Drossel et al., 2001, 2004), the Tangled-nature model (Christensen et al., 2002; Hall et al., 2002; di Collobiano et al., 2003), and simplified versions of the latter (Rikvold and Zia, 2003; Zia and Rikvold, 2004; Sevim and Rikvold, submitted), as well as the network models due to Chowdhury et al. (2003) (Chowdhury and Stauffer, 2005, and references therein). These models are all deliberately quite simple, aiming to elucidate *universal* features that are largely independent of the finer details of the ecological interactions and the evolutionary mechanisms. Such universal features may include lifetime distributions for species and communities, as well as other aspects of extinction statistics, statistical properties of fluctuations in diversity and population sizes, and the structure and dynamics of food webs that develop and change on both the ecological and evolutionary time scales. By changing specific features of the various simplified models, one hopes to learn which aspects of the models are linked to the observed properties of the resulting communities and their development with time.

In this paper we discuss a class of such models, which combine features from all of the ones mentioned above. We first define the class in general, and then proceed to study, by linear stability analysis and large-scale Monte Carlo simulations, specific members of the class. These contain simplifying features that enable us to obtain several analytical results. A main conclusion is that the time-averaged size of the total population for each of these simplified models can be mapped onto what is known as a ϕ^3 model in the theory of phase transitions and critical phenomena. However, in contrast to other systems that can be formulated in this framework, the model parameters in the systems studied here are not fixed by external constraints (such as temperature or magnetic field in physical or chemical examples), but rather *evolve* in such a way as to maximize a *community fitness function*, subject only to constraints internal to the model. The models are thus *self-optimizing*, and kinetic Monte Carlo simulations show that several quantities that characterize the self-optimized state, such as the total population, the diversity, and the lifetimes of partic-

ular species and of evolutionarily quiet periods, are described by power-law distributions. However, in contrast to some popular species-based models of macroevolution (Bak and Sneppen, 1993; Newman and Palmer, 2003, and references therein), it is not clear if the self-optimized state is also a critical state in the sense of statistical mechanics.

The rest of this paper is organized as follows. The general class of models is introduced in Sec. 2. In Sec. 3 we introduce simplifications that make the models amenable to analytical linear stability analysis. Such analysis is performed, and the results are compared with large-scale kinetic Monte Carlo simulations. Additional simulation results that go beyond the mean-field approximation inherent in the linear stability analysis are presented in Sec. 4. A concluding summary is presented in Sec. 5, and some technical details of the derivation of the community fitness function are discussed in the Appendix.

2 General Model

The models studied here are simplified population-dynamics models, similar to multispecies Lotka-Volterra models (Murray, 1989), that are augmented to enable evolution of new species through a mutation mechanism. The models are defined as follows.

Individual organisms that belong to a particular species (the species is indicated by the label I) reproduce asexually at the end of each generation, each giving rise to F offspring individuals with probability P_I before dying. With probability $(1 - P_I)$, they die without offspring. No individual thus survives beyond one generation. (For simplicity, the fecundity F will be assumed fixed, independent of both species and individual. In fact, all individuals of a particular species are assumed to be identical in every way.) The species are characterized by a “genome” consisting of a string of L “binary genes” (“bits”) that can each take one of the two alleles, 0 or 1. There are thus 2^L potential species. However, typically only a few of these potential species are present in the community at any one time.

During reproduction, each gene in an offspring individual’s genome may undergo mutation ($0 \rightarrow 1$ or $1 \rightarrow 0$) with a small probability μ/L (typically, $\mu = 10^{-3}$ is used in the simulations). A mutated individual is assumed to belong to a completely different species than its parent, with entirely different properties. This is clearly a highly idealized picture. However, previous work (Sevim and Rikvold, submitted) indicates that a model, in which species that differ only by one or a few bits have similar properties, nevertheless has long-time dynamical properties very similar to the model studied by Rikvold and Zia (2003). That model, like the ones studied here, has no

correlations between the properties of closely related species. [See, however, discussion by Tokita and Yasutomi (2003).]

The reproduction probability $P_I(t)$ for an individual of species I in generation t depends on the individual's ability to utilize the amount of external resources available, R , and on its interactions with the population sizes $n_J(t)$ of all the species present in the community at that time. [We emphasize that the population size $n_J(t)$ is the number of individuals of species J in generation t . It is thus restricted to being an integer ≥ 0 .] The dependence of P_I on the set of n_J is determined by an *interaction matrix* \mathbf{M} (Solé et al., 1996) with elements $M_{IJ} \in [-1, 1]$ in a way defined specifically in the next paragraph. If M_{IJ} is positive and M_{JI} is negative, then I is a predator and J its prey, and *vice versa*. If both matrix elements are positive, the species interact in a *mutualistic* way, while both elements negative implies direct competition. The matrix \mathbf{M} is *independent of time*.

Specifically, the reproduction probability for species I , $P_I(t)$, depends on R and the set $\{n_J(t)\}$ through the nonlinear form,

$$P_I(t) = \frac{1}{1 + \exp[-\Delta_I(R, \{n_J(t)\})]} , \quad (1)$$

where

$$\Delta_I(R, \{n_J(t)\}) = -b_I + \eta_I R f_1 + \sum_J M_{IJ} f_2 g_2 n_J(t) - N_{\text{tot}}(t)/N_0 . \quad (2)$$

Here b_I can be seen as the “energy cost” of reproduction (always positive), and η_I (positive for primary producers or autotrophs, and zero for consumers or heterotrophs) is the ability of individuals of species I to utilize the external resource R . The factors f_1 and f_2 are functions of the population sizes that represent competition for resources (f_1) or prey (f_2), and g_2 is a function that expresses the ability of a predator to engage in adaptive foraging (Drossel et al., 2004). The total population size is $N_{\text{tot}}(t) = \sum_J n_J(t)$. [In contrast, the total number of *species* present in generation t (the species richness) will be defined as $\mathcal{N}(t)$.] The constant N_0 is a Verhulst factor (Verhulst, 1838; Murray, 1989), perhaps due to some shared resource such as space. It plays the role of an environmental carrying capacity that prevents the population size from diverging to infinity. For large positive Δ_I (small birth cost, strong coupling to the external resources, more prey than predators, and a total population size that does not significantly exceed N_0), the individual almost certainly reproduces, giving rise to F offspring. In the opposite limit of large negative Δ_I (large birth cost, weak or no coupling to the external resources, more predators than prey, and/or a total population size that significantly exceeds N_0), it almost certainly dies without offspring. The nonlinear depen-

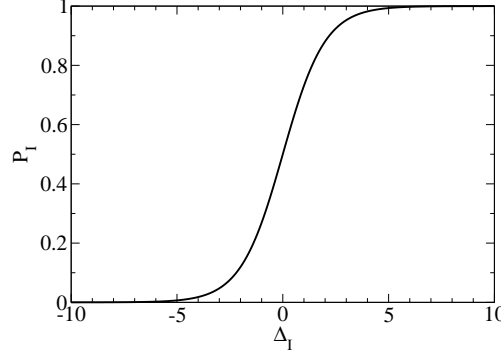


Fig. 1. The dependence of the reproduction probability for an individual of species I , P_I , on the value of the function $\Delta_I(R, \{n_J\})$, defined in Eq. (2). The nonlinear form of P_I ensures both that the reproduction probability does not exceed unity, even under extremely favorable conditions (large positive Δ_I), and that there exists a practical negative limit on Δ_I , below which conditions are so unfavorable that reproduction is virtually impossible.

dence of P_I on Δ_I thus limits the growth rate of the population size, even under extremely favorable conditions. It also sets a practical negative limit on Δ_I , below which conditions are so unfavorable that reproduction is virtually impossible. The dependence of P_I on Δ_I is shown in Fig. 1. The reproduction probability P_I , together with the specific form of its argument, $\Delta_I(R, \{n_J\})$, play the role of a functional response for this class of models (Drossel et al., 2001; Krebs, 2001, Chs. 13–14). The model parameters are chosen to represent the realistic situation that the number of species that exist in the community at any time is much smaller than the number of potential species (i.e., that $\mathcal{N}(t) \ll 2^L$), and also that $\mathcal{N}(t) \ll N_{\text{tot}}(t)$.

An analytic approximation describing the development in time of the mean values of the population sizes, $\langle n_I(t) \rangle$, can be written as a set of coupled difference equations,

$$\begin{aligned} \langle n_I(t+1) \rangle &= \langle n_I(t) \rangle F P_I(R, \{\langle n_J(t) \rangle\}) [1 - \mu] \\ &+ (\mu/L) F \sum_{K(I)} \langle n_{K(I)}(t) \rangle P_{K(I)}(R, \{\langle n_J(t) \rangle\}) + O(\mu^2), \end{aligned} \quad (3)$$

where $K(I)$ is the set of species that can be generated from species I by a single mutation (“nearest neighbors” of I).

3 Simplified Models

A very simple choice of parameters in Eq. (2) is $f_1 = f_2 = 1/N_{\text{tot}}(t)$ and $g_2 = 1$. This represents universal competition and absence of adaptive foraging, and

so is not a very realistic choice. However, it has the advantage that it turns Eq. (3) in the absence of mutations (i.e., with $\mu = 0$) into a set of linear equations for the population sizes in a fixed-point community. This set can be solved analytically to give the average population size of each species, as well as the average total population size and the stability properties of the community. In this paper we consider specifically two such simplified models, which can serve as benchmarks for future studies of models involving more realistic choices of f_1 , f_2 , and g_2 .

3.1 Model A

The first of these models, which we here call Model A, is the one introduced and studied in great detail by Rikvold and Zia (2003). [See also Zia and Rikvold (2004); Sevim and Rikvold (submitted).] In this model, the M_{IJ} for $I \neq J$ are stochastically independent and uniformly distributed on $[-1, +1]$, while the intra-species interactions $M_{II} = 0$. The external resource R and the reproduction costs b_I are all equal to zero, and the total population size $N_{\text{tot}}(t)$ is limited only by the Verhulst factor N_0 . The numerical results presented here are for $N_0 = 2000$, $F = 4$, $L = 13$, and $\mu = 10^{-3}$. These are the same parameters used by Rikvold and Zia (2003).

3.2 Model B

The second model, here called Model B, is a predator-prey model. This is implemented by making the off-diagonal part of \mathbf{M} antisymmetric. In order to keep the connectance of the resulting communities consistent with food webs observed in nature (Dunne et al., 2002; Garlaschelli, 2004, and references therein), the (M_{IJ}, M_{JI}) pairs are chosen nonzero with probability $c = 0.1$. The nonzero M_{IJ} are chosen independently and uniformly on $[-1, +1]$. This model does not have a Verhulst term [i.e., formally, $N_0 = \infty$ in Eq. (2)], and the community is supported by a constant external resource, R . Only a proportion p of the 2^L potential species are producers that can directly utilize the resource (for the numerical data reported here, we use $p = 0.05$). Thus, with probability $(1 - p)$ the resource coupling $\eta_I = 0$, representing consumers, while with probability p the η_I are independently and uniformly distributed on $(0, +1]$, representing producers of varying efficiency. In addition to the constraints on \mathbf{M} mentioned above, we require that producers ($\eta_I > 0$) always are the prey of consumers ($\eta_I = 0$). The population sizes are limited by independent reproduction costs b_I that are uniformly distributed on $(0, +1]$, and by negative intra-species interactions M_{II} independently and uniformly distributed on $[-1, 0)$. The numerical results presented here are for $R = 2000$,

$F = 2$, $L = 13$, and $\mu = 10^{-3}$. (Our rationale for the choices of F in the two models will be discussed in Sec. 3.4 below.)

Some numerical results for Model B were presented by Rikvold (2005a). An extensive numerical study will be published elsewhere (Rikvold, 2005b).

3.3 Fixed-point communities

To obtain the stationary solution of Eq. (3) with $\mu = 0$ for a community of \mathcal{N} species, we must require $P_I = 1/F$ for all \mathcal{N} species. Equations (1) and (2) then give rise to the \mathcal{N} linear relations

$$-\tilde{b}_I + \eta_I \frac{R}{N_{\text{tot}}^*} + \sum_J M_{IJ} \frac{n_J^*}{N_{\text{tot}}^*} - \frac{N_{\text{tot}}^*}{N_0} = 0 , \quad (4)$$

where $\tilde{b}_I = b_I - \ln(F - 1)$. (For simplicity, we have dropped the $\langle \rangle$ notation for the average population sizes, and the asterisk superscripts denote fixed-point solutions.) In a convenient vector notation, $|n^*\rangle$ is the column vector composed of the \mathcal{N} nonzero n_I^* , while $\langle 1|$ is an \mathcal{N} -dimensional row vector composed entirely of ones. Thus, the total population size is given by the inner product, $N_{\text{tot}}^* = \langle 1|n^*\rangle = \sum_I n_I^*$, and Eq. (4) takes the matrix form

$$-\tilde{b} \rangle N_{\text{tot}}^* + R|\eta\rangle + \hat{\mathbf{M}}|n^*\rangle - |1\rangle(N_{\text{tot}}^*)^2/N_0 = 0 . \quad (5)$$

Here, $|\tilde{b}\rangle$ is the column vector whose elements are \tilde{b}_I , $|\eta\rangle$ is the column vector whose elements are η_I (in both cases including only those \mathcal{N} species that have nonzero n_I^*), $\hat{\mathbf{M}}$ is the corresponding $\mathcal{N} \times \mathcal{N}$ submatrix of \mathbf{M} , and $|1\rangle$ is an \mathcal{N} -dimensional column vector of ones. The solution for $|n^*\rangle$ is

$$|n^*\rangle = -\hat{\mathbf{M}}^{-1} \left[|\eta\rangle R - |\tilde{b}\rangle N_{\text{tot}}^* - |1\rangle(N_{\text{tot}}^*)^2/N_0 \right] , \quad (6)$$

where $\hat{\mathbf{M}}^{-1}$ is the inverse of $\hat{\mathbf{M}}$. To find each n_I^* , we must first obtain $N_{\text{tot}}^* \equiv \langle 1|n^*\rangle$. Multiplying Eq. (6) from the left by $\langle 1|$, we obtain the quadratic equation

$$R\mathcal{E} - \Theta N_{\text{tot}}^* - (N_{\text{tot}}^*)^2/N_0 = 0 . \quad (7)$$

The coefficients,

$$\Theta = \frac{\langle 1|\hat{\mathbf{M}}^{-1}|\tilde{b}\rangle - 1}{\langle 1|\hat{\mathbf{M}}^{-1}|1\rangle} \quad \text{and} \quad \mathcal{E} = \frac{\langle 1|\hat{\mathbf{M}}^{-1}|\eta\rangle}{\langle 1|\hat{\mathbf{M}}^{-1}|1\rangle} , \quad (8)$$

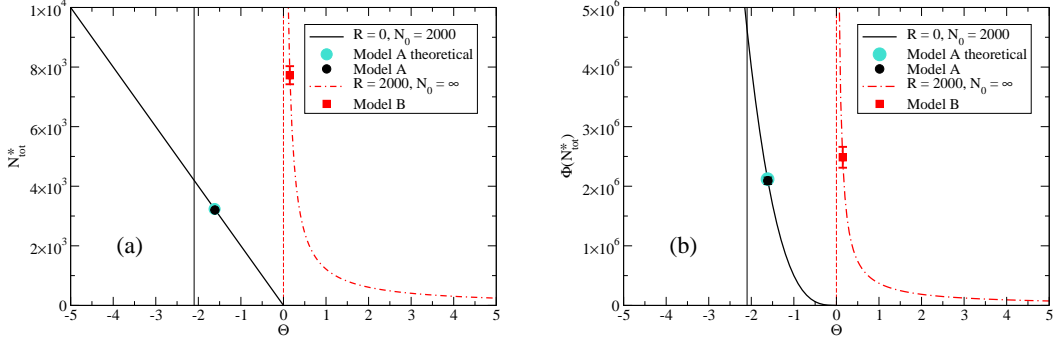


Fig. 2. (Color online.) Results of the mean-field approximation for (a) The total fixed-point population size N_{tot}^* and (b) the community fitness function $\Phi(N_{\text{tot}}^*)$. Both are shown vs Θ for fixed $\mathcal{E} = 0.61$. The solid vertical lines represent the absolute minimum value for Θ in Model A, while the dotted vertical lines represent the analogous limit for Model B. The points marked “Model A” and “Model B” were obtained from large-scale Monte Carlo simulations as described in the text. The calculation of the point marked “Model A theoretical” is also described in the text.

can be viewed as an effective interaction strength and an effective coupling to the external resource, respectively. Approximate expressions for Θ and \mathcal{E} that are less accurate but more intuitive are obtained in the Appendix. The nonnegative solution of Eq. (7) is

$$N_{\text{tot}}^* = -\frac{\Theta N_0}{2} + \sqrt{\left(\frac{\Theta N_0}{2}\right)^2 + R\mathcal{E}N_0}. \quad (9)$$

Figure 2(a) shows N_{tot}^* as a function of Θ for two choices of N_0 and R at fixed \mathcal{E} . Special cases of the solution are

$$N_{\text{tot}}^* = \begin{cases} -\Theta N_0 & \text{for } R = 0 \quad \text{and} \quad \Theta \leq 0 \\ 0 & \text{for } R = 0 \quad \text{and} \quad \Theta \geq 0 \\ \sqrt{R\mathcal{E}N_0} & \text{for } \Theta = 0 \quad \text{and} \quad \mathcal{E} \geq 0 \\ R\mathcal{E}/\Theta & \text{for } N_0 = \infty \text{ and/or } \langle 1|\hat{\mathbf{M}}^{-1}|1 \rangle = 0 \end{cases}. \quad (10)$$

To find each n_I^* separately, we now only need to insert the solution for N_{tot}^* in Eq. (6).

Only those $|n^*\rangle$ that have all positive elements can represent a *feasible* community (Roberts, 1974). If $\hat{\mathbf{M}} = \mathbf{0}$, the set of equations (5) is inconsistent for $\mathcal{N} > 1$, unless \tilde{b}_I and η_I both are independent of I (this case is equivalent to $\mathcal{N} = 1$). The only possible stationary community then consists of one single species, the one with the largest value of η_I/\tilde{b}_I . This result is an example of competitive exclusion (Hardin, 1960; Armstrong and McGehee, 1980;

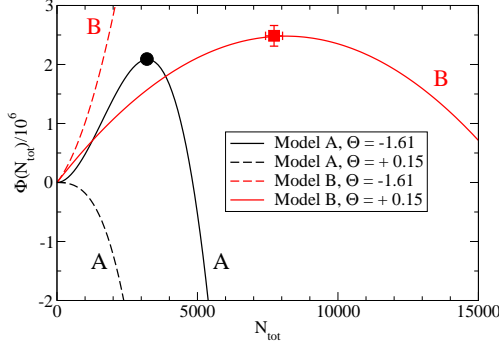


Fig. 3. (Color online.) The community fitness function $\Phi(N_{\text{tot}})$, shown vs N_{tot} for Model A (black) and Model B (gray, red online). For Model A the parameters are: $F = 4$, $R = 0$, and $N_0 = 2000$. For Model B they are: $F = 2$, $R = 2000$, $\mathcal{E} = 0.61$, and $N_0 = \infty$. The values of Θ used are -1.61 , corresponding to the average value taken by Model A in the simulations, and $+0.15$, corresponding to the average value taken by Model B. $\Phi(N_{\text{tot}})$ has a nontrivial maximum for Model A at negative Θ (solid black curve marked A), and for Model B at positive Θ (solid gray curve marked B (red online)). The circular and square data points are the results of Monte Carlo simulations and correspond to the equally shaped points in Fig. 2. They lie very close to the maximum of $\Phi(N_{\text{tot}})$ for each model. The dashed curves show the physically inaccessible cases of Model A with $\Theta > 0$ (stable, absorbing state at $N_{\text{tot}} = 0$) and Model B with $\Theta < 0$ (monotonically increasing $\Phi(N_{\text{tot}})$).

den Boer, 1986).

Equation (7) can be seen as a maximization condition for a “community fitness” function,

$$\Phi(N_{\text{tot}}) = \left(1 - \frac{1}{F}\right) \left(R\mathcal{E}N_{\text{tot}} - \frac{\Theta}{2}N_{\text{tot}}^2 - \frac{1}{3N_0}N_{\text{tot}}^3 \right). \quad (11)$$

The dependence of Φ on N_{tot} is shown in Fig. 3 for Models A and B at two different values of Θ . Here we have obtained Eq. (11) simply by integration of Eq. (7). A conventional mean-field derivation, which also explains the prefactor $(1-1/F)$ and provides intuitive approximations for Θ and \mathcal{E} , is given in the Appendix. The maximum value of Φ with respect to N_{tot} , $\Phi(N_{\text{tot}}^*)$, is shown vs Θ for two different values of N_0 at fixed \mathcal{E} in Fig. 2(b). Because of the term cubic in N_{tot} in Eq. (11), the class of models described by this equation are known as ϕ^3 models. They have a critical point at $\Theta = 0$ and $R = 0$. For negative values of Θ there exists a spontaneously populated phase, in which N_{tot}^* is positive, even for $R = 0$. A finite Verhulst factor N_0 is then needed to keep the population size from diverging to infinity. This class of models describes systems that have a phase transition involving an *absorbing state* (here, the state with $n_I = 0$ for all I). [For readers with a background in phase transitions and critical phenomena we note that such absorbing models are known to belong to the universality class of directed percolation (Janssen et al., 1999;

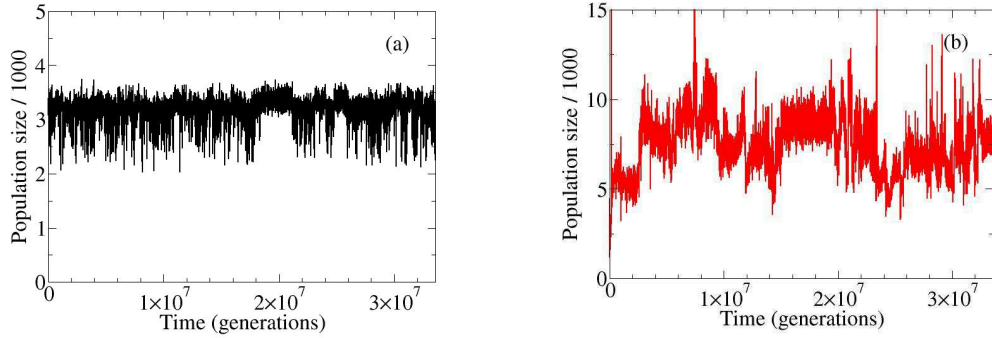


Fig. 4. (Color online.) Typical time series of the total population sizes, $N_{\text{tot}}(t)$, for Monte Carlo runs of $2^{25} = 33\,554\,432$ generations each. To reduce the size of the figure file, the data are sampled only once every 2048 generations. While this slightly reduces the apparent range of the short-time fluctuations, the general shapes of the time series are preserved. (a) Model A: $N_0 = 2000$, $R = 0$, $F = 4$, $L = 13$, and $\mu = 10^{-3}$. (b) Model B: $N_0 = \infty$, $R = 2000$, $F = 2$, $L = 13$, and $\mu = 10^{-3}$.

Hinrichsen, 2000).] Other examples include models of epidemics, poisoning of catalytic processes, certain autocatalytic chemical reactions, and lasers. The spontaneously populated phase that occurs for negative Θ is only accessible if the interaction matrix allows mutualistic interactions (i.e., M_{IJ} and M_{JI} both positive). In contrast, predator-prey interactions (an antisymmetric interaction matrix) limit the system to nonnegative Θ , for which external resources are required to maintain a positive population size. In the absence of mutations and extinctions, Θ and \mathcal{E} are constant. However, mutations enable the community not only to maximize $\Phi(N_{\text{tot}})$ for fixed parameters, *but also to increase it further as new, favorable mutations appear*. Numerically we find that the community progresses toward the minimum value of Θ (and thus the maximum value of $\Phi(N_{\text{tot}}^*)$) compatible with the constraints on \mathbf{M} and $|\tilde{b}\rangle$. Whether this point is a critical point in a larger space of variables that include Θ and \mathcal{E} , remains an open question.

In Monte Carlo simulations of Model A (in which the offdiagonal elements of \mathbf{M} are uncorrelated and uniformly distributed on $[-1, +1]$), it was found that the community spent most of its time in a succession of quasi-steady states (QSS), separated by brief bursts of intense evolutionary activity (Rikvold and Zia, 2003). All the QSS studied in detail were found to be mutualistic, with $\overline{M_{IJ}} = 0.78 \pm 0.03$ and $\overline{\Theta} = -1.61 \pm 0.01$. [Here, the overbar represents averages over all the ten QSS listed in Table I of Rikvold and Zia (2003).] The average of N_{tot} , taken over all the 16 realizations of 2^{25} generations that were studied, was $\overline{N_{\text{tot}}} = 3201 \pm 8$. (The average over only the ten QSS agrees with the total average to within the statistical errors, showing that the periods when the system is not in a QSS contribute negligibly to the overall time averages.) In Fig. 2(a), $\overline{N_{\text{tot}}}$ is shown vs $\overline{\Theta}$ as a black dot, while the corresponding value of $\Phi(\overline{N_{\text{tot}}})$ is shown in Fig. 2(b). A typical time series of $N_{\text{tot}}(t)$ for Model A is

included in Fig. 4(a).

We can also obtain a theoretical estimate for the point $(\overline{\Theta}, \overline{N_{\text{tot}}})$ in Model A. Assuming for simplicity that all the nondiagonal M_{IJ} have the same value, a , using the definition of Θ , and remembering that in this case $F = 4$, so that $\tilde{b}_I = -\ln 3$ for all I , one can show that $\Theta = -[(1 - 1/\mathcal{N})a + \ln 3]$, where \mathcal{N} is the total number of species in the community. This yields the absolute minimum value for Θ equal to $-(1 + \ln 3) \approx -2.10$ for $\mathcal{N} = \infty$ (shown by vertical full lines in Fig. 2). However, it was shown by Rikvold and Zia (2003) that the most probable number of species in a community is $\mathcal{N}^\dagger \approx L \ln 2 / \ln(1/q)$, where q is the probability of finding a pair of interactions, M_{IJ} and M_{JI} , conducive to this community. With M_{IJ} randomly distributed on $[-1, +1]$, the probability of drawing a pair that are both larger than a value m , is $q = [(1 - m)/2]^2$. While retaining our approximate formula for Θ , we now replace \mathcal{N} by \mathcal{N}^\dagger with this value of q , and a by $(1 + m)/2$, which is the average of a variable uniformly distributed over $[m, 1]$. This yields

$$\Theta \approx - \left\{ \left[1 - \frac{2 \ln \left(\frac{2}{1-m} \right)}{13 \ln 2} \right] \frac{1+m}{2} + \ln 3 \right\} \quad (12)$$

for $L = 13$. This is a concave function of m with a single minimum at m_{min} , which can be found numerically. The result is $m_{\text{min}} \approx 0.512$, which yields $\Theta_{\text{min}} \approx -1.618$, $N_{\text{tot}} \approx 3236$, and $\overline{M_{IJ}} = (1 + m_{\text{min}})/2 \approx 0.756$. These values are in excellent agreement with those obtained from the Monte Carlo simulations, and they are shown as gray dots (turquoise online) in Fig. 2.

The results for Model B that are included in Fig. 2 were also obtained from Monte Carlo simulations of 2^{25} generations, the details of which will be reported elsewhere (Rikvold, 2005b). The parameter values used in the figure were extracted as the average values from thirteen QSS communities identified in twelve independent simulation runs: $\overline{\mathcal{E}} = 0.61 \pm 0.04$ and $\overline{\Theta} = 0.15 \pm 0.01$. The value of the total population size given in the figure is the total time average over the simulations, averaged over all twelve runs, $\overline{N_{\text{tot}}} = 7726 \pm 303$. (Like for Model A, averages over only the particular observed QSS communities agree with this total average to within the error bars.) The large uncertainty in $\overline{N_{\text{tot}}}$ in this case is a direct consequence of the steep slope of the phase diagram for Model B for values of $\overline{\Theta}$ closely above its critical value of zero.

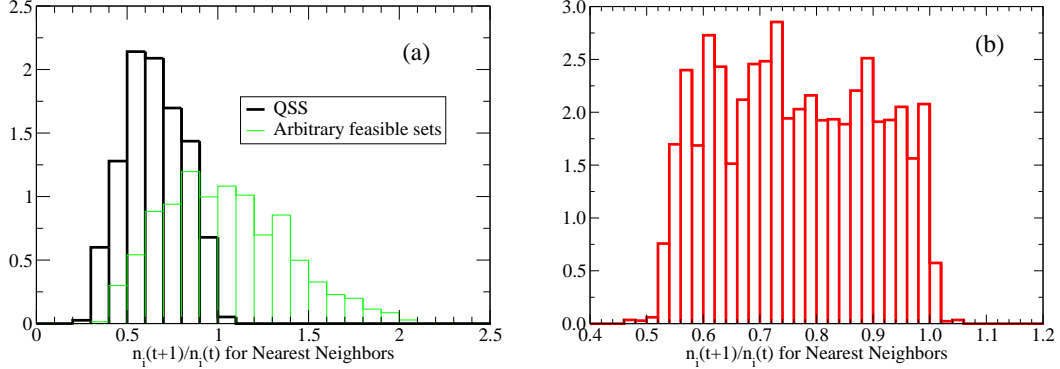


Fig. 5. (Color online.) Normalized histograms of the invader growth rates (exponential of the invasion fitness) for nearest-neighbor species of a QSS community for both models. **(a)** Histograms for Model A, based on the ten specific QSS included in Table I of Rikvold and Zia (2003) (thick, black lines), compared with the results for arbitrary, feasible, and internally stable communities [thin, gray lines (green online)]. After Rikvold and Zia (2003). **(b)** Histograms based on thirteen QSS communities identified from simulations of Model B. For this model, all randomly selected communities that we tried turned out to be both unfeasible and internally unstable – a sign that feasible and internally stable communities must be much rarer in this predator/prey system, than in the mutualistic Model A.

3.4 Stability of fixed-point community

The internal stability of an \mathcal{N} -species fixed-point community is obtained from the matrix of partial derivatives,

$$\left. \frac{\partial n_I(t+1)}{\partial n_J(t)} \right|_{|n^* \rangle} = \delta_{IJ} + \Lambda_{IJ} , \quad (13)$$

where δ_{IJ} is the Kronecker delta function and Λ_{IJ} are elements of the *community matrix* Λ (Murray, 1989). Straightforward differentiation yields

$$\Lambda_{IJ} = \left(1 - \frac{1}{F}\right) \frac{n_I^*}{N_{\text{tot}}^*} \left[M_{IJ} - \frac{R\eta_I + (\hat{\mathbf{M}}|n^* \rangle)_I}{N_{\text{tot}}^*} - \frac{1}{N_0} \right] , \quad (14)$$

where $(\hat{\mathbf{M}}|n^* \rangle)_I$ is the element of the column vector $\hat{\mathbf{M}}|n^* \rangle$, corresponding to species I . In order for deviations from the fixed point to decay monotonically in magnitude, the real parts of the eigenvalues of the matrix of partial derivatives in Eq. (13), $\Lambda + \mathbf{1}$ where $\mathbf{1}$ is the \mathcal{N} -dimensional unit matrix, must lie in the interval $(-1, +1)$. The values of the fecundity F that are used in this work (4 for Model A and 2 for Model B) were chosen to satisfy this requirement for $\mathcal{N} = 1$.

Since new species are created by mutations, we must also study the stability of the fixed-point community toward “invaders.” Consider a mutant invader i . Then its multiplication rate, in the limit that $n_i \ll n_J$ for all \mathcal{N} species J in the resident community, is given by

$$\frac{n_i(t+1)}{n_i(t)} = \frac{F}{1 + \exp[-\Delta_i(R, \{n_J^*\})]} . \quad (15)$$

The Lyapunov exponent, $\ln[n_i(t+1)/n_i(t)]$, is the *invasion fitness* of the mutant with respect to the resident community (Metz et al., 1992; Doebeli and Dieckmann, 2000). A characteristic feature of the QSS communities observed in both Model A and Model B is that very few of the mutants that are separated from the resident community by a single mutation (“nearest-neighbor species”) have multiplication rates above unity. In fact, this is true only to a slightly lesser degree for mutants separated by two or three mutations from the resident species (“next-nearest neighbors” and “third-nearest neighbors”). Thus, a string of rather unsuccessful mutations is necessary to bring significant change to a QSS community – a fact that to a large extent accounts for their high degree of stability. This effect is illustrated for both models in Fig. 5.

4 Comparison of Dynamical Features

In this section we go beyond the mean-field treatment of the previous sections to compare some of the dynamical features observed in long kinetic Monte Carlo simulations of Model A and Model B. These simulations and their results were described in detail for Model A by Rikvold and Zia (2003), and a detailed discussion for Model B will be reported elsewhere (Rikvold, 2005b). For both models we performed multiple simulations of $2^{25} = 33\,554\,432$ generations with a genome of length $L = 13$ ($2^{13} = 8192$ potential species) and a mutation rate of $\mu = 10^{-3}$. The fecundity F was set to 4 for Model A and 2 for Model B.

In addition to the total population sizes shown in Fig. 4, we also studied the diversities of the resulting communities, defined as the number of (major) resident species. In order to obtain an approximation for the number of major species [which can be thought of as the wildtypes in a quasi-species model (Eigen, 1971; Eigen et al., 1988)], we here filter out the low-population species that are most likely unsuccessful mutants of the wildtypes. This is achieved by using the exponential Shannon-Wiener diversity index (Krebs, 1989),

$$D(t) = e^{S[\{n_I(t)\}]} , \quad (16)$$

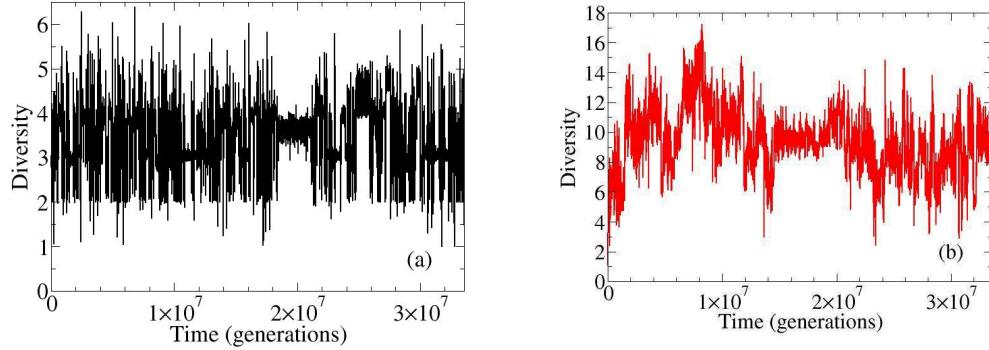


Fig. 6. (Color online.) Typical time series of the exponential Shannon-Wiener diversity index $D(t)$ in the same 2^{25} -generations Monte Carlo runs shown in Fig. 4. To reduce the size of the figure file, the data were downsampled as in Fig. 4. **(a)** Model A. **(b)** Model B.

where

$$S[\{n_I(t)\}] = - \sum_{\{I|\rho_I(t) > 0\}} \rho_I(t) \ln \rho_I(t) \quad (17)$$

with $\rho_I(t) = n_I(t)/N_{\text{tot}}(t)$ is the information-theoretical entropy (Shannon, 1948; Shannon and Weaver, 1949). Typical time series for $D(t)$ in the two models are shown in Fig. 6. Just like in the time series for the total population sizes, the intermittent structure consisting of QSS on different timescales, separated by periods of high evolutionary activity, is clearly seen.

Statistical information for several characteristic times that describe the dynamics can be extracted from our data. One such time is the duration of a QSS. One way to determine this is to use a cutoff on the size of the diversity fluctuations, whose probability densities for the two models are shown in Fig. 7(a). In both cases, the probability densities consist of a Gaussian central part representing the fluctuations during the QSS periods (Zia and Rikvold, 2004), flanked by “wings” that correspond to the large fluctuations during the evolutionarily active periods. Based on the data in this figure we choose a cutoff $y_c = 0.015$ for Model A and 0.010 for Model B. The duration of a single QSS then corresponds to the time interval between consecutive times when $|\text{d}S(t)/\text{d}t|$ exceeds y_c . Log-log plots of the resulting probability densities for the durations of QSS in the two models are shown together in Fig. 7(b). While both show approximate power-law behavior over five decades or more in time, there is an important difference: the power-law exponent for Model A is near -2 , while for Model B it is closer to -1 .

A different time of interest is the lifetime of a particular species, defined as the time elapsed between its origination and eventual extinction. Log-log plots of histograms of the species lifetimes in the two models are shown in Fig. 8. In

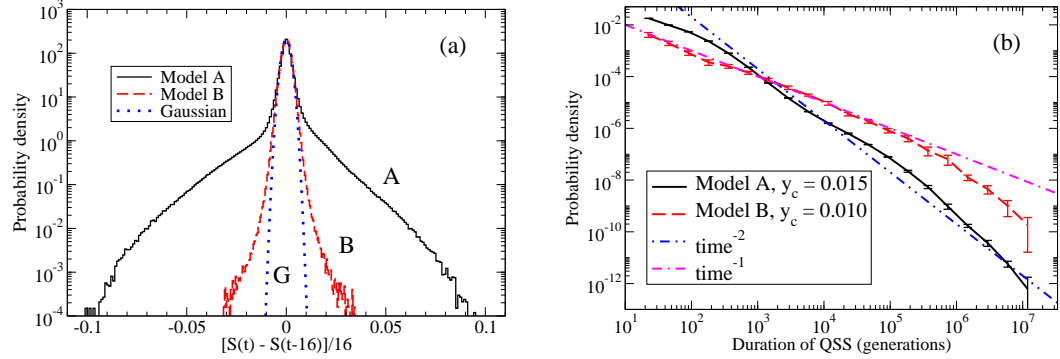


Fig. 7. (Color online.) (a) Normalized histograms representing the probability density of the logarithmic derivative of the diversity, $dS(t)/dt$. The data were averaged over 16 generations in each run, and then averaged over 16 independent runs for Model A (solid, marked A) and 12 runs for Model B (dashed, marked B). The central parts of both histograms are well fitted by the *same* Gaussian distribution (dotted, marked G). After Rikvold (2005a). (b) Log-log plot of normalized histograms representing the probability density of the durations of QSS, estimated as the periods between times when $|dS(t)/dt|$ exceeds a cutoff y_c ($dS(t)/dt$ was averaged over 16 generations as in part (a)). Model A (solid) and Model B (dashed). Results for Model A were averaged over 16 runs, and for Model B over 12 runs. The error bars are standard errors, based on the spread between runs. The two dot-dashed straight lines represent time^{-2} and time^{-1} power laws, respectively. After Rikvold (2005a).

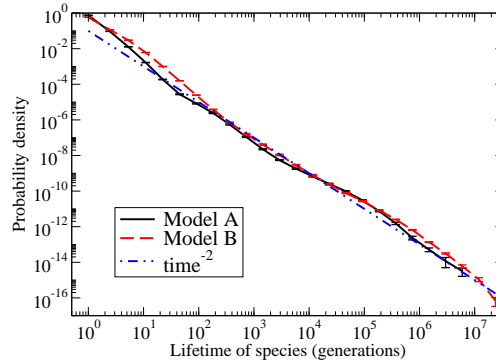


Fig. 8. (Color online.) Log-log plot of normalized histograms representing the probability density of the lifetime of a particular species. Model A (solid) and Model B (dashed). Results for Model A were averaged over eight runs, and for Model B over 12 runs. The error bars were calculated as in Fig. 7(b). The dot-dashed straight line represents a time^{-2} power law. After Rikvold (2005a).

contrast to the case of the QSS durations, the species-lifetime distributions are very close for the two models, both showing approximate time^{-2} behavior over near seven decades in time. The observed exponent is significantly different from $-3/2$, which would correspond to the simple hypothesis that the lifetime distributions simply correspond to the first-return-time distribution for a random walk of n_I (Newman and Palmer, 2003, Ch. 1). Lifetime

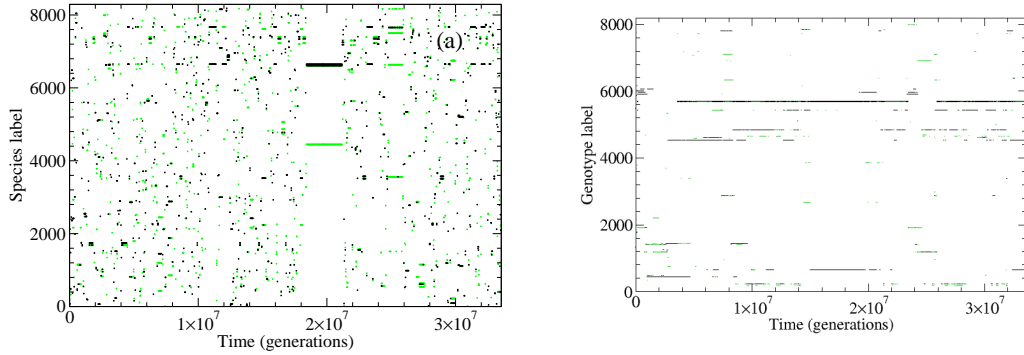


Fig. 9. (Color online.) Plots showing the labels I of the most highly populated species vs time. The data are for the same 2^{25} -generation Monte Carlo runs shown in Figs. 4 and 6. Gray (green online): $n_I \in [101, 1000]$. Black: $n_I \geq 1001$. (a) Model A. (b) Model B. For clarity, only producer species are shown for this model. The consumer species give a similar picture (Rikvold, 2005b). See further discussion in the text.

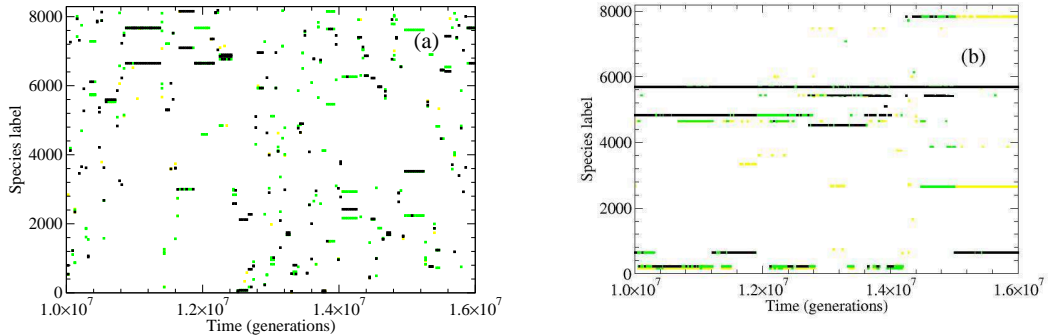


Fig. 10. (Color online.) Magnified version of Fig. 9, showing times between 1.0×10^7 and 1.6×10^7 generations. In addition to the species shown in Fig. 9, the ones with $n_I \in [11, 100]$ are also shown (light gray, yellow online). (a) Model A. (b) Model B. See further discussion in the text.

distributions for marine genera that are compatible with a power law with an exponent in the range -1.5 to -2 have been obtained from the fossil record (Newman and Sibani, 1999; Newman and Palmer, 2003, Ch. 1). However, the possible power-law behavior in the fossil record is only observed over about one decade in time – between 10 and 100 million years – and other fitting functions, such as exponential decay, are also possible. Nevertheless, it is reasonable to conclude that the numerical results obtained from complex, interacting evolution models that extend over a large range of time scales support interpretations of the fossil lifetime evidence in terms of nontrivial power laws.

The difference in the power laws for the QSS durations and the species lifetimes is a puzzling result. One possible explanation can be gleaned from the data shown in Figs. 9 and 10. These show the species labels of highly populated

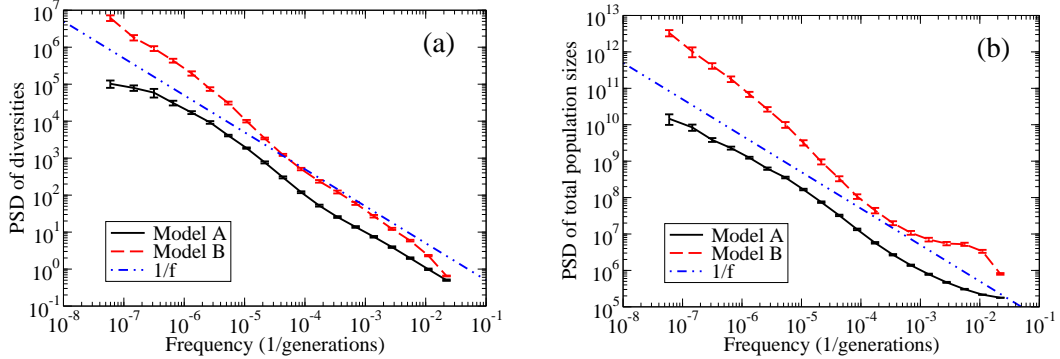


Fig. 11. (Color online.) Log-log plots of PSDs of (a) the diversities $D(t)$ and (b) the total population sizes $N_{\text{tot}}(t)$ for Model A and Model B. The PSDs are averaged over each octave in frequency, and then over 16 runs for Model A and 12 runs for Model B. The error bars were calculated as in Fig. 7(b). The dashed straight lines represent $1/f$ power-law behavior.

species as functions of time for both models. From Figs. 9(a) and 10(a) it is seen that all or most of the horizontal lines representing populated species at a given time for Model A start and stop almost simultaneously, indicating that species originations and extinctions for this model are highly synchronized. In other words: whole communities in Model A tend to go extinct and be replaced with an entirely new community within a short time. In contrast, in Figs. 9(b) and 10(b) the different horizontal species lines for Model B stop and start at different times. This indicates that communities in this model are much more robust, and extinction events seldom wipe out more than a part of the total community. Thus, QSS would be expected to be more long-lived (but also less clearly defined) for Model B, than for Model A.

The arbitrariness inherent in the cutoff that must be used to extract QSS duration distributions from fluctuations in the diversity or other time series can to some extent be eliminated by mapping distributions obtained with different cutoffs onto a common scaling function (Paczuski et al., 1996; Rikvold, 2005a). However, an analysis method that completely avoids any cutoffs is that of calculating power spectral densities (the square of the temporal Fourier transform). Power spectra (PSDs) are therefore shown in Fig. 11 for both models. The PSDs for the diversity are shown in Fig. 11(a), and for the total population size in Fig. 11(b). Although there are clear deviations, the overall behaviors for both quantities and for both models are compatible with a $1/f$ power law over many decades in frequency. In the high-frequency regime the population-size PSDs have a significant background of noise, presumably caused by the rapid population fluctuations due to the birth and death of individual organisms. For very low frequencies there is little reason to believe that there should be large differences between the behaviors of the two quantities for the same model. We therefore think it is reasonable to consider the difference between the slopes of the diversity and population-size PSDs for

Model A as an indication of the true uncertainty in the PSDs at the lowest frequencies. Better estimates in this regime would require orders of magnitude longer simulations.

5 Discussion and Conclusions

In this paper we have introduced a class of individual-based models of biological coevolution, and we have shown that a simplified subclass of these models is amenable to analytic linear stability calculations. Since the simplification involves universal competition and ignores important effects such as adaptive foraging, the resulting models are not highly realistic. However, the fact that the results of numerical simulations can be compared with analytical results make these simplified models ideal as benchmarks for simulations of more realistic models in the future.

The central result of the analytic study is the fact that, in the absence of mutations, the total population size of a fixed-point community, N_{tot}^* , can be mapped onto the order parameter of a model of phase transitions with an absorbing state. This type of phase-transition model is called a ϕ^3 model and belongs to the universality class of directed percolation. In addition to the present application, the ϕ^3 model is also applicable to phase transitions in such diverse systems as epidemics, lasers, and autocatalytic chemical reactions. However, the evolution models studied here differ from those kinds of systems by the important effect that, in the *presence* of mutations, the model parameters Θ and \mathcal{E} are no longer externally imposed constraints, but rather *evolve* as far in the direction of negative Θ as allowed by the internal constraints of the particular model. As a result, Model A, in which the elements of the interspecies interaction matrix \mathbf{M} are randomly distributed on an interval that is symmetric about zero, evolves to produce communities that are heavily biased toward mutualism. The effective interaction variable Θ adjusts to a negative value, where a community of nonzero population size can spontaneously occur *without* an external resource. In contrast, the predator/prey Model B, in which the interspecies interactions are antisymmetric, is constrained to nonnegative values of Θ , for which a nonzero population size can only be sustained through an external resource. These results are illustrated in Fig. 2(a). In the analogy with thermal phase transitions suggested by the ϕ^3 model, Θ appears as a temperature-like variable with negative values corresponding to subcritical temperatures and positive values corresponding to supercritical temperatures.

In a recent study of a similar, but different model for coevolution, Tokita and Yasutomi (2003) also observed the emergence of strongly mutualistic communities from initially unbiased conditions. In their model, mutants are very similar to their

parents, except for their interactions with a few other species (“local mutations” in the words of those authors), and they suggest that the evolution of mutualism is related to this feature of their model. However, the mutations in our models would be “global” in the language of Tokita and Yasutomi, which leads us to the conclusion that the emergence of mutualism is common in models where mutualistic interactions are allowed. In fact, we have seen little difference in the dynamics between the version of Model A studied in this paper and a version with strongly correlated, and thus more “local,” interactions (Sevim and Rikvold, submitted). It remains an important problem to reconcile this tendency for evolution of mutualism with the obvious requirement that biomass cannot be created without energy input. While predator/prey interactions are easy to reconcile with energy conservation, mutualistic interactions (although they are common in nature (Kawanabe et al., 1993; Bronstein, 1994; Krebs, 2001, Ch. 14)) are more difficult to interpret in an energy framework.

Beyond the mean-field studies and the simulation results for average population sizes, we have also studied the temporal fluctuations of both the diversity and total population size for Models A and B. We find that the probability distributions of the lifetimes of individual species in both models are very similar, showing power-law decay with an exponent near -2 over near seven decades in time, as seen in Fig. 8. [This exponent value is consistent with some interpretations of the available data for the lifetimes of marine genera in the fossil record (Newman and Sibani, 1999; Newman and Palmer, 2003, Ch. 1), but other interpretations of the fossil evidence are also possible.] Similarly, power spectra for the diversity, as well as for the total population size, show reasonable (although not perfect) $1/f$ behavior over many decades in frequency, as seen in Fig. 11. It is therefore very interesting that the probability distributions of the durations of individual QSS periods in the two models also both show reasonable power-law decay, but with *different* exponents: near -2 for Model A and close to -1 for Model B, as seen in Fig. 7(b). This result, which we found quite surprising at first, makes sense in light of the observation that the extinctions of major species are highly synchronized in Model A, while they are much less so in Model B. While communities in Model A tend to collapse completely when an aggressive mutant arrives and/or a major species goes extinct, communities in Model B are much more resilient and extinctions most often only extend to one or a few branches of the resident food web. This effect is illustrated in Figs. 9 and 10.

Our observation of the high resilience of Model B against complete extinction of communities is consistent with observations of extinction avalanches of limited size in the Web-world model by Drossel et al. (2001), who argue that their model is therefore *not* self-organized critical. Together with our observation of the self-optimization of the class of evolution models studied here to points *away from* the critical point of the ϕ^3 model, these observations may support a conclusion that models of coevolution that take reasonable account

of the dynamics at the ecological level (even if they are extremely simplified) are not in general self-organized critical. Such a conclusion would be in disagreement with a number of recent theories of extinction (Bak and Sneppen, 1993; Newman and Palmer, 2003, and references therein). On the other hand, it is also possible that the stationary states achieved by the systems studied here may represent critical points in a larger variable space than that of the fixed-parameter ϕ^3 model.

Since it is difficult to measure the size of extinction avalanches in our models without an arbitrary coarse-graining of time, we have not performed direct measurements of avalanche-size distributions to compare with the results of Drossel et al. (2001). However, power spectra of the intensity of extinction in one single generation show approximate $1/f$ noise in the low-frequency regime, similar to the PSDs of diversities and total population sizes and indicative of very long time correlations of extinction events [Fig. 4(b) of Rikvold (2005a)]. The same reference also gives tentative arguments that the exponents observed for Model B (but not for Model A) may be interpreted to agree with scaling-theory expectations for the universality class of the self-organized critical Bak-Sneppen extinction model in *zero* spatial dimensions (Paczuski et al., 1996; Dorogovtsev et al., 2000). Thus, it appears that recent work on models of macroevolution that are based on events on ecological time scales by now raise as many intriguing questions as they answer about the long-time dynamics of biological evolution. Further work on such models, with comparisons of the results with data from the fossil record, as well as from laboratory experiments and extant food webs, is clearly desirable. In a forthcoming paper we will consider in detail the structure and dynamics of the food webs that develop within Model B (Rikvold, 2005b).

Acknowledgments

The author thanks R. K. P. Zia, B. Schmittmann, P. Beerli, G. J. P. Naylor, and V. Sevim for useful discussions and comments on the manuscript, and V. Sevim for the data on Model A included in Fig. 8. He also gratefully acknowledges hospitality at Kyoto University by H. Tomita in the Department of Fundamental Sciences, Faculty of Integrated Human Studies, and H. Fujisaka in the Department of Applied Analysis and Complex Dynamical Systems, Graduate School of Informatics.

This work was supported in part by U.S. National Science Foundation Grants No. DMR-0240078 and DMR-0444051, and by Florida State University through the School of Computational Science, the Center for Materials Research and Technology, the National High Magnetic Field Laboratory, and a COFRS summer-salary grant.

A Mean-field Derivation of ϕ^3 Community Fitness Function

In this Appendix we provide a conventional derivation of the ϕ^3 form of the community fitness function $\Phi(N_{\text{tot}})$ in a simple mean-field approximation. The derivation provides an explanation for the prefactor $(1 - 1/F)$ in Eq. (11), as well as intuitively clear approximations for the coefficients Θ and \mathcal{E} . It also provides justification that the equation to be integrated to obtain $\Phi(N_{\text{tot}})$ is indeed Eq. (7), rather than this equation multiplied or divided by some power of N_{tot} . The derivation is based on the time-dependent Ginzburg-Landau equation for a system with nonconserved order parameter (Hohenberg and Halperin, 1977; Goldenfeld, 1992, Ch. 8.3), which for our current systems takes the form

$$\frac{\partial N_{\text{tot}}}{\partial t} = \frac{\partial \Phi}{\partial N_{\text{tot}}}. \quad (\text{A.1})$$

(The fitness Φ is the negative of the Landau free energy customarily considered in physics applications.)

Identifying $\partial n_I(t)/\partial t$ with $n_I(t+1) - n_I(t)$, we obtain from Eqs. (1–3) in the absence of mutations:

$$\frac{\partial n_I(t)}{\partial t} = n_I(t) \left\{ \frac{F}{1 + \exp \left[b_I - \frac{\eta_I R}{N_{\text{tot}}(t)} - \sum_J M_{IJ} \frac{n_J(t)}{N_{\text{tot}}(t)} + \frac{N_{\text{tot}}(t)}{N_0} \right]} - 1 \right\}. \quad (\text{A.2})$$

Expanding this nonlinear equation of motion around its fixed point, we get

$$\frac{\partial n_I(t)}{\partial t} \approx \left(1 - \frac{1}{F}\right) n_I(t) \left[-\tilde{b}_I + \frac{\eta_I R}{N_{\text{tot}}(t)} + \sum_J M_{IJ} \frac{n_J(t)}{N_{\text{tot}}(t)} - \frac{N_{\text{tot}}(t)}{N_0} \right]. \quad (\text{A.3})$$

To obtain the simplest mean-field approximation for $\partial N_{\text{tot}}/\partial t$ (exact for $\mathcal{N} = 1$), we set $n_I \approx N_{\text{tot}}/\mathcal{N}$, $\tilde{b}_I \approx \mathcal{N}^{-1} \sum'_I \tilde{b}_I \equiv \langle \tilde{b} \rangle$, $\eta_I \approx \mathcal{N}^{-1} \sum'_I \eta_I \equiv \langle \eta \rangle$, and $M_{IJ} \approx \mathcal{N}^{-2} \sum'_{IJ} M_{IJ} \equiv \langle M \rangle$, where the primes on the sums indicate that they are restricted to the \mathcal{N} species with $n_I > 0$. This yields

$$\frac{\partial N_{\text{tot}}}{\partial t} \approx \left(1 - \frac{1}{F}\right) \left[R\langle\eta\rangle - (\langle\tilde{b}\rangle - \langle M \rangle) N_{\text{tot}} - \frac{(N_{\text{tot}})^2}{N_0} \right]. \quad (\text{A.4})$$

Integrating the right-hand side as prescribed by Eq. (A.1), we find

$$\Phi(N_{\text{tot}}) \approx \left(1 - \frac{1}{F}\right) \left(R\langle\eta\rangle N_{\text{tot}} - \frac{\langle\tilde{b}\rangle - \langle M \rangle}{2} N_{\text{tot}}^2 - \frac{1}{3N_0} N_{\text{tot}}^3 \right). \quad (\text{A.5})$$

This result has the same cubic form as Eq. (11), with the approximate coefficients $\langle \eta \rangle \approx \mathcal{E}$ and $(\langle \tilde{b} \rangle - \langle M \rangle) \approx \Theta$. The exact fixed-point solution for N_{tot} requires the use of \mathcal{E} and Θ , but the approximate forms obtained here provide a more intuitive understanding of the significance of these coefficients.

References

Armstrong, R. A., McGehee, R., 1980. Competitive exclusion. *Am. Naturalist* 115, 151–170.

Bak, P., Sneppen, K., 1993. Punctuated equilibrium and criticality in a simple model of evolution. *Phys. Rev. Lett.* 71, 4083–4086.

Bronstein, J. L., 1994. Our current understanding of mutualism. *Quart. Rev. Biol.* 69, 31–51.

Caldarelli, G., Higgs, P. G., McKane, A. J., 1998. Modelling coevolution in multispecies communities. *J. theor. Biol.* 193, 345–358.

Chowdhury, D., Stauffer, D., 2005. Evolutionary ecology in-silico: Does mathematical modelling help in understanding the generic trends? *J. Biosciences* 30, 277–287.

Chowdhury, D., Stauffer, D., Kunwar, A., 2003. Unification of small and large time scales for biological evolution: Deviations from power law. *Phys. Rev. Lett.* 90, 068101.

Christensen, K., di Collobiano, S. A., Hall, M., Jensen, H. J., 2002. Tangled-nature: A model of evolutionary ecology. *J. theor. Biol.* 216, 73–84.

den Boer, P. J., 1986. The present status of the competitive exclusion principle. *Trends Ecol. Evol.* 1, 25–28.

di Collobiano, S. A., Christensen, K., Jensen, H. J., 2003. The tangled nature model as an evolving quasi-species model. *J. Phys. A* 36, 883–891.

Doebeli, M., Dieckmann, U., 2000. Evolutionary branching and sympatric speciation caused by different types of ecological interactions. *Am. Naturalist* 156, S77–S101, and references therein.

Dorogovtsev, S. N., Mendes, J. F. F., Pogorelov, Y. G., 2000. Bak-Sneppen model near zero dimension. *Phys. Rev. E* 62, 295–298.

Drossel, B., Higgs, P. G., McKane, A. J., 2001. The influence of predator-prey population dynamics on the long-term evolution of food web structure. *J. theor. Biol.* 208, 91–107.

Drossel, B., McKane, A., Quince, C., 2004. The impact of non-linear functional responses on the long-term evolution of food web structure. *J. theor. Biol.* 229, 539–548.

Dunne, J., Williams, R. J., Martinez, N. D., 2002. Network structure and diversity loss in food webs: Robustness increases with connectance. *Ecol. Lett.* 5, 558–567.

Eigen, M., 1971. Selforganization of matter and evolution of biological macromolecules. *Naturwissenschaften* 58, 465.

Eigen, M., McCaskill, J., Schuster, P., 1988. Molecular quasi-species. *J. Phys. Chem.* 92, 6881–6891.

Garlaschelli, D., 2004. Universality in food webs. *Eur. Phys. J. B* 38, 277–285.

Goldenfeld, N., 1992. Lectures on Phase Transitions and the Renormalization Group. Addison-Wesley, Reading, MA.

Hall, M., Christensen, K., di Collobiano, S. A., Jensen, H. J., 2002. Time-dependent extinction rate and species abundance in a tangled-nature model of biological evolution. *Phys. Rev. E* 66, 011904.

Hardin, G., 1960. The competitive exclusion principle. *Science* 131, 1292–1297.

Hinrichsen, H., 2000. Nonequilibrium critical phenomena and phase transitions into absorbing states. *Adv. Phys.* 49, 815–958.

Hohenberg, P. C., Halperin, B., 1977. Theory of dynamic critical phenomena. *Rev. Mod. Phys.* 49, 435–479.

Janssen, H. K., Kuttbay, Ü., Oerding, K., 1999. Equation of state for directed percolation. *J. Phys. A* 32, 1809–1817.

Kawanabe, H., Cohen, J. E., Iwasaki, K., 1993. Mutualism and Community Organization. Oxford University Press, Oxford.

Krebs, C. J., 1989. Ecological Methodology. Harper & Row, New York, Chap. 10.

Krebs, C. J., 2001. Ecology. The Experimental Analysis of Distribution and Abundance. Fifth Edition. Benjamin Cummings, San Francisco.

Metz, J. A. J., Nisbet, R. M., Geritz, S. A. H., 1992. How should we define ‘fitness’ for general ecological scenarios? *Trends Ecol. Evol.* 7, 198–202.

Murray, J. D., 1989. Mathematical Biology. Springer-Verlag, Berlin.

Newman, M. E. J., Palmer, R. G., 2003. Modeling Extinction. Oxford University Press, Oxford.

Newman, M. E. J., Sibani, P., 1999. Extinction, diversity and survivorship of taxa in the fossil record. *Proc. R. Soc. Lond. B* 266, 1583–1599.

Paczuski, M., Maslov, S., Bak, P., 1996. Avalanche dynamics in evolution, growth, and depinning models. *Phys. Rev. E* 53, 414–443.

Rikvold, P. A., 2005a. Fluctuations in models of biological macroevolution. In: Kish, L. B., Lindenberg, K., Gingl, Z. (Eds.), Noise in Complex Systems and Stochastic Dynamics III. SPIE, The International Society for Optical Engineering, Bellingham, WA, pp. 148–155. E-print arXiv:q-bio.PE/0502046.

Rikvold, P. A., 2005b. Fluctuations and food webs in an individual-based predator/prey model of biological coevolution. In preparation.

Rikvold, P. A., Zia, R. K. P., 2003. Punctuated equilibria and $1/f$ noise in a biological coevolution model with individual-based dynamics. *Phys. Rev. E* 68, 031913.

Roberts, A., 1974. The stability of a feasible random ecosystem. *Nature (London)* 251, 607–608.

Sevim, V., Rikvold, P. A., submitted to *J. Phys. A*. Effects of correlated interactions in a biological coevolution model with individual-based dynamics. E-print arXiv:q-bio.PE/0507040.

Shannon, C. E., 1948. A mathematical theory of communication. *Bell Syst.*

Tech. J. 27, 379–423, 628–656.

Shannon, C. E., Weaver, W., 1949. The Mathematical Theory of Communication. University of Illinois Press, Urbana.

Solé, R. V., Bascompte, J., Manrubia, S., 1996. Extinction: Bad genes or weak chaos? *Proc. R. Soc. Lond. B* 263, 1407–1413.

Thompson, J. N., 1998. Rapid evolution as an ecological process. *Trends Ecol. Evol.* 13, 329–332.

Thompson, J. N., 1999. The evolution of species interactions. *Science* 284, 2116–2118.

Tokita, K., Yasutomi, A., 2003. Emergence of a complex and stable network in a model ecosystem with extinction and mutation. *Theor. Popul. Biol.* 63, 131–146.

Verhulst, P. F., 1838. Notice sur la loi que la population suit dans son accroissement. *Corres. Math. et Physique* 10, 113–121.

Yoshida, T., Jones, L. E., Ellner, S. P., Fussmann, G. F., Hairston, N. G., 2003. Rapid evolution drives ecological dynamics in a predator-prey system. *Nature* 424, 303–306.

Zia, R. K. P., Rikvold, P. A., 2004. Fluctuations and correlations in an individual-based model of biological coevolution. *J. Phys. A* 37, 5135–5155.